*Hydrological Processes*

WILEY

RESEARCH ARTICLE OPEN ACCESS

# Parameterizing Haverkamp Model From the Steady-State of Numerically Generated Infiltration: Influence of Algorithms for Steady-State Selection

Dario Autovino[1] | Vincenzo Bagarello[1] | Massimo Iovino[1] | Laurent Lassabatere[2] | Deniz Yilmaz[3,4]

[1]Department of Agricultural, Food and Forest Sciences, University of Palermo, Palermo, Italy | [2]University of Lyon, Université Claude Bernard Lyon 1, CNRS, ENTPE, UMR 5023 LEHNA, Vaulx-en-Velin, France | [3]Université Grenoble Alpes, CNRS, IRD, Grenoble INP, IGE, Grenoble, France | [4]Engineering Faculty, Civil Engineering Department, Munzur University, Tunceli, Turkey

**Correspondence:** Vincenzo Bagarello (vincenzo.bagarello@unipa.it)

**Received:** 17 June 2024 | **Revised:** 18 October 2024 | **Accepted:** 22 October 2024

**Funding:** This work was supported by RETURN Extended Partnership and received funding from the European Union Next-GenerationEU (National Recovery and Resilience Plan—NRRP, Mission 4, Component 2, Investment 1.3—D.D. 1243 2/8/2022, PE0000005).

**Keywords:** analytical infiltration models | BEST methods of soil hydraulic characterization | numerically simulated infiltration | saturated soil hydraulic conductivity | sorptivity

## ABSTRACT

BEST (Beerkan Estimation of Soil Transfer parameters) methods of soil hydraulic characterisation are widely applied for estimating sorptivity, $S$, and saturated hydraulic conductivity, $K_s$. Calculating these properties requires choosing the $\beta$ and $\gamma$ parameters of the Haverkamp infiltration model. These parameters can be obtained from numerically simulated three-dimensional (3D) infiltration runs reaching steady-state. This investigation tested dependence of the estimated $\beta$ and $\gamma$ parameters on the algorithm for steady-state selection using simulated 3D cumulative infiltrations for different soils and initial conditions. Two algorithms used the original simulation outputs and included using (i) a threshold defining steadiness (T-algorithm) and (ii) the last four data points, yielding a reference value of steady-state infiltration rate (R-algorithm). A third algorithm, similar to the R-algorithm, was applied to previously re-sampled infiltration data at fixed time intervals (RR-algorithm). The intercept, $b_s$, of the straight line fitted to the data describing steady-state on the cumulative infiltration plot depended on the applied algorithm more than the slope of this line. Consequently, $\beta$ varied with the applied algorithm more than $\gamma$. The RR-algorithm, yielding $0.62 \leq \beta \leq 1.99$ and $0.74 \leq \gamma \leq 0.98$, was preferred since it mediated between advantages and disadvantages of T- and R-algorithms. The influence of the choice of proper values for $\beta$ and $\gamma$ on the estimates of $S$ and $K_s$ was evaluated using BEST. Using the default values of $\beta$ (0.6) and $\gamma$ (0.75) yielded accurate estimates of $S$ but not of $K_s$. Soil dependent $\beta$ and $\gamma$ values should be used in this case. A check of the reliability of the estimates of $b_s$ can be made by a sequential analysis of the cumulative infiltration data. Future developments include considering sources differing in size and establishing if the suggested $\beta$ and $\gamma$ values apply in general to the available BEST algorithms.

## 1 | Introduction

Soil loss due to water erosion is a natural and unavoidable phenomenon that can however become excessive, and hence intolerable, in particular situations and mostly due to anthropic factors (Pimentel 2006). Soil erosion occurs when water does not enter the soil and instead moves on the soil surface. Soil water repellency represents a key factor in post-fire erosion (Doerr, Shakesby, and Macdonald 2009). Soil erosion processes are strongly affected by rainfall partition into infiltration

and surface runoff. This partition depends on many factors including, with a central role, soil hydrodynamic properties. Understanding and modelling soil erosion process, especially by physical models, requires adequately characterising the soil from a hydrodynamic point of view. There are various methodologies for determining soil hydrodynamic properties either in the field or in the laboratory. Field methods are more onerous since many replications of the experiment have to be performed in environmental conditions that are not always favourable to appropriately characterise an area of interest. However, they are considered preferable over laboratory methods since the functional connection of the conductive pore system with the surrounding medium is guaranteed only in the former case. Field infiltration methods have gained a large popularity for determining soil hydrodynamic properties since they are relatively simple, rapid and cost-effective (Angulo-Jaramillo et al. 2016). These experiments involve establishing an infiltration process from a small-diameter circular source onto an initially unsaturated soil. Due to their versatility, these methodologies have been applied in a wide range of natural and anthropogenic soils (Angulo-Jaramillo et al. 2019; Yilmaz et al. 2019).

The three-dimensional (3D) infiltration model by Haverkamp et al. (1994) has received much interest from the scientific community over the years and has led, amongst other things, to development in 2006 of a simple field method to completely characterise the soil, that is to simultaneously estimate the soil water retention and hydraulic conductivity curves. The method, named BEST—Beerkan Estimation of Soil Transfer parameters, requires performing an infiltration experiment at a null ponded depth of water on the soil surface and collecting some additional information on particle size distribution, initial and final soil water content and dry soil bulk density (Lassabatère et al. 2006). Pedotransfer functions are used to estimate the shape parameters of the soil water retention and hydraulic conductivity curves. Measurement of water infiltration yields the scale parameters of these curves. Different algorithms, that is BEST-slope, BEST-intercept and BEST-steady, can be used to analyse the infiltration data (Lassabatère et al. 2006; Yilmaz et al. 2010; Bagarello, Di Prima, and Iovino 2014; Angulo-Jaramillo et al. 2016, 2019). BEST methods of analysis of a field measured infiltration curve have recently been adapted for use in water repellent soils (Di Prima et al. 2021), implying that these methods are very appropriate for soil hydraulic characterisation in relevant contexts for studying water erosion processes.

Using BEST methods of soil hydraulic characterisation requires making a choice about the values assumed by the two shape parameters of the infiltration model, $\beta$ and $\gamma$. Commonly, $\beta = 0.6$ and $\gamma = 0.75$ is assumed for practical use of BEST methods (Lassabatère et al. 2006; Angulo-Jaramillo et al. 2016) since Haverkamp et al. (1994) suggested to use these two values as reliable means. However, Haverkamp et al. (1999, 2005) later considered the shape parameters as dependent on both the soil and the initial soil water content (Lassabatere et al. 2009). According to several investigations, $\beta$ can be expected to vary between 0.33 and 1.56 and $\gamma$ from 0.75 to 1.03 (Lassabatere et al. 2009; Moret-Fernández and Latorre 2017; Moret-Fernández et al. 2020; Rahmati et al. 2020).

Yilmaz et al. (2023) recently developed a new procedure to simultaneously determine $\beta$ and $\gamma$ from numerically simulated 3D infiltration runs reaching steady-state conditions. Their approach makes use of the long-time expansion of the infiltration model by Haverkamp et al. (1994) and the exact soil properties, that is soil sorptivity, $S$ [L/T$^{0.5}$], and saturated soil hydraulic conductivity, $K_s$ [L/T]. The slope, $i_s$ [L/T], and the intercept, $b_s$ [L], of the straight line fitted to the data describing steady-state conditions on the cumulative infiltration, $I$ [L], versus time, $t$ [T], plot have to be determined for calculating $\beta$ and $\gamma$. Yilmaz et al. (2023) too recognised that these parameters vary with both the soil and the initial soil water content but they also proposed, for initially dry soil conditions, some fixed values instead of those currently used ($\beta = 0.6$; $\gamma = 0.75$; Haverkamp et al. 1994; Lassabatère et al. 2006). In particular, using 0.9 for both constants was suggested for coarse-textured soils. For finer soils, $\gamma = 0.75$ can generally be considered. Soils with an intermediate permeability can be characterised with $\beta = 0.75$ whereas $\beta = 1.5$ should be used for little permeable soils.

To detect attainment of steady-state conditions during the infiltration process, Yilmaz et al. (2023) adapted an algorithm, originally developed by Bagarello, Iovino, and Reynolds (1999) and Bagarello and Giordano (1999), that was denoted here as T-algorithm (T = threshold). Briefly, a reference slope is initially calculated by linear regression of the last four ($I$ and $t$) data points. Then, going backward during the run, an additional data point is considered for the linear regression and the percentage difference between the new estimate of $i_s$ and the reference $i_s$ value is calculated. The procedure is applied repeatedly by adding each time an additional ($I$ and $t$) data point and it stops when the new $i_s$ value differs from the reference $i_s$ value by more than a threshold, fixed at 0.5% by Yilmaz et al. (2023). In this backward procedure, the first ($I$ and $t$) data point yielding a percentage difference higher than 0.5% represents the last data point of the transient stage. All the subsequent ($I$ and $t$) data points during the run are considered expressive of the steady-state stage and they are used to determine $i_s$ and $b_s$ and hence $\beta$ and $\gamma$.

In principle, the procedure applied by Yilmaz et al. (2023) provides an objective estimate of the duration of the transient stage of the infiltration process and, being based on a large number of data points, it is appropriate to capture trends in the case of experimental data with errors or that of numerically generated data with oscillations and dispersions. However, it also exposes the analysis to the risk of improperly treating transient data as expressive of flow steadiness with the consequence of overestimating $i_s$ and underestimating $b_s$.

For an infiltration run of a given duration, this last risk is minimised if the last four data points of the $I$ vs. $t$ curve are considered (Yilmaz et al. 2023) since these data are expressive of the process at the most advanced stage possible (R-algorithm; R = reference). It is currently unknown if and to what extent the estimates of $\beta$ and $\gamma$ change when the T- and the R-algorithms are applied to the same run.

Typically, numerically simulated infiltration curves comprise a large number of data points. In practise, however, infiltration is often sampled at fixed time intervals, that might also be relatively long in advanced stages of the runs, or by reading the

time when a fixed water volume has infiltrated. With these methods, the infiltration run could be described by a relatively limited number of data points. For example, 8–15 ($I$ and $t$) data pairs could fully describe an infiltration curve obtained by a Beerkan run (Braud et al. 2005; Lassabatère et al. 2006). A given steady-state attainment criterion could therefore be applied to a run described at a different level of detail, depending on the circumstances. It is necessary to also establish if the estimated $\beta$ and $\gamma$ values change depending on the number of data points describing the sampled infiltration process.

The general objective of this investigation was to obtain robust estimates of the shape parameters of the Haverkamp infiltration model, usable for predicting soil sorptivity and saturated soil hydraulic conductivity with the BEST methods. Considering different soils (from sand to silt) under different initial saturation degrees not exceeding 0.4, the specific objectives were to: (i) establish the effect of the used algorithm to assess flow steadiness on estimation of the $\beta$ and $\gamma$ parameters; (ii) determine the dependence of these two parameters on the time interval at which simulated infiltration data are acquired and their dependence upon initial conditions; and (iii) derive $\beta$ and $\gamma$ values usable to obtain accurate estimates of $S$ and $K_s$ in different soils.

## 2 | Materials and Methods

### 2.1 | BEST-Steady

The BEST-steady algorithm yields the following estimates of soil sorptivity, $S$ (mm/h$^{0.5}$), and saturated soil hydraulic conductivity, $K_s$ (mm/h) (Bagarello, Di Prima, and Iovino 2014; Angulo-Jaramillo et al. 2016, 2019):

$$S = \sqrt{\frac{i_s}{A + \frac{C}{b_s}}} \tag{1}$$

$$K_s = \frac{C\, i_s}{A\, b_s + C} \tag{2}$$

in which $i_s$ (mm/h) and $b_s$ (mm) are the slope and the intercept, respectively, of the straight line fitted to the data describing steady-state conditions on the cumulative infiltration, $I$ (mm), versus time, $t$ (h), plot. The $A$ (1/mm) and $C$ (–) constants are defined as:

$$A = \frac{\gamma}{r\left(\theta_s - \theta_i\right)} \tag{3}$$

$$C = \frac{1}{2(1-\beta)\left(1 - \frac{K_i}{K_s}\right)} ln\left(\frac{1}{\beta}\right) \tag{4}$$

where $\gamma$ is a shape parameter for geometrical correction of the infiltration front shape, $r$ (mm) is the radius of the source, $\theta_s$ (m$^3$/m$^3$) is the volumetric soil water content at saturation, $\theta_i$ (m$^3$/m$^3$) is the initial volumetric soil water content, $\beta$ is a shape parameter varying with the soil type and the initial soil water content (Lassabatere et al. 2009) and $K_i$ (mm/h) is the soil hydraulic conductivity corresponding to a volumetric soil water content equal to $\theta_i$. Note that these equations are derived from the asymptotic approximate expansion of the Haverkamp infiltration model, which analytically computes cumulative infiltration in both transient and steady states (Haverkamp et al. 1994).

### 2.2 | Determining $\beta$ and $\gamma$ From a Steady-State Beerkan Run

According to Yilmaz et al. (2023), the values of $\gamma$ and $\beta$, treated as unknown parameters, can be obtained from a 3D infiltration run reaching steady-state conditions. In particular, $\gamma$ is given by:

$$\gamma = \frac{r\left(\theta_s - \theta_i\right)\left(i_s - K_s\right)}{S^2} \tag{5}$$

whereas $\beta$ can be determined by finding the zero for the following function:

$$f(\beta) = b_s - \frac{S^2}{2(1-\beta)\left(K_s - K_i\right)} ln\left(\frac{1}{\beta}\right) \tag{6}$$

The two equations, Equations (5) and (6), can be derived from the BEST-steady Equations (1–4). In particular, combining Equations (1) and (2) yields:

$$C = b_s \frac{K_s}{S^2} \tag{7}$$

Substituting Equation (7) into Equation (4) yields Equation (6). Solving Equations (1) and (2) for $A$ and using Equation (7) for $C$ yields:

$$A = \frac{i_s}{S^2} - \frac{C}{b_s} = \frac{C}{b_s}\left(\frac{i_s}{K_s} - 1\right) = \frac{i_s - K_s}{S^2} \tag{8}$$

Substituting Equation (8) into Equation (3) and solving for $\gamma$ gives Equation (5).

### 2.3 | Numerically Simulated Infiltration Data

The same numerical simulations performed by Yilmaz et al. (2023) were used in this investigation. In particular, 3D infiltration was simulated for sandy (Sa), loamy-sand (LoSa), sandy-loam (SaLo), loam (Lo), silty-loam (SiLo) and silty (Si) soils. The van Genuchten (1980) model and the related soil hydraulic properties (Carsel and Parrish 1988) were used for these simulations (Table 1).

Data were obtained for a circular source with a radius $r = 50$ mm, a null ponded depth of water on the infiltration surface and different values of the initial saturation degree, $S_{ei} = (\theta_i - \theta_r)/(\theta_s - \theta_r)$, in which $\theta_i$ (m$^3$/m$^3$), $\theta_r$ (m$^3$/m$^3$) and $\theta_s$ (m$^3$/m$^3$) are the initial, residual and saturated volumetric soil water contents, respectively (Table 2). For each soil, the highest $\theta_i/\theta_s$ ratio was close to 0.4–0.5 and, overall, the ratio between the initial soil hydraulic conductivity, $K_i$ (mm/h), and $K_s$ did not exceed $8.36 \times 10^{-3}$ (Table 2). The theoretical sorptivity, $S$ (mm/h$^{0.5}$), calculated for each soil and each $S_{ei}$ value according to Lassabatere

**TABLE 1** | Soil hydraulic parameters (Carsel and Parrish 1988) and duration, $t_{sim}$, of the numerically simulated infiltration runs.

| Soil | $\theta_s$ (m³/m³) | $\theta_r$ (m³/m³) | $n$ | $\alpha$ (1/cm) | $K_s$ (mm/h) | $t_{sim}$ (h) |
|---|---|---|---|---|---|---|
| Sand (Sa) | 0.43 | 0.045 | 2.68 | 0.145 | 297.0 | 0.5 |
| Loamy-sand (LoSa) | 0.41 | 0.057 | 2.28 | 0.124 | 145.9 | 1.0 |
| Sandy-loam (SaLo) | 0.41 | 0.065 | 1.89 | 0.075 | 44.2 | 2.0 |
| Loam (Lo) | 0.43 | 0.078 | 1.56 | 0.036 | 10.4 | 4.0 |
| Silty-loam (SiLo) | 0.45 | 0.067 | 1.41 | 0.02 | 4.5 | 8.0 |
| Silt (Si) | 0.46 | 0.034 | 1.37 | 0.016 | 2.5 | 12.0 |

*Note:* $\theta_s$ = volumetric soil water content at saturation; $\theta_r$ = residual volumetric soil water content; $n$ and $\alpha$ = empirical parameters of the van Genuchten (1980) model for the water retention curve; $K_s$ = saturated soil hydraulic conductivity.

et al. (2023), was also provided by Yilmaz et al. (2023) and was reported in Table 2.

The duration of the simulations, $t_{sim}$ (h), varied with the soil from 0.5 h for the Sa soil to 12 h for the Si soil (Table 1). The maximum simulation time was fixed large enough by Yilmaz et al. (2023) to reach steady-state. For each run, a cumulative infiltration vs. time curve was obtained for both transient and steady states. The number of ($I$ and $t$) data pairs for a run varied from a minimum of 203 (LoSa soil, $S_{ei} = 0.4$) to a maximum of 866 (Si soil, $S_{ei} = 0$). From these numerically generated data, we then extrapolated ($I$ and $t$) data pairs for specific times. In particular, the original infiltration outputs of the numerical simulations were resampled according to the following practical criterion: every minute for the first 30 min, every 2 min up to 60 min, every 5 min up to 120 min, and every 15 min up to 720 min. The aim was to obtain infiltration curves similar, in terms of time interval between readings, to those that could be plausible to obtain in the field. In this case, the number of data pairs for a run varied between 30 (Sa soil) and 97 (Si soil).

## 2.4 | Calculations and Data Analysis

In this investigation, three algorithms were applied to determine the slope, $i_s$, and the intercept, $b_s$, of the straight line fitted to the data describing steady-state conditions on the cumulative infiltration plot and hence to calculate $\beta$ and $\gamma$ by Equations (6) and (5), respectively. An application example of these three algorithms to one of the runs considered in this investigation is shown in Figure 1.

With the R-algorithm (R = reference), $i_s$ and $b_s$ were obtained by linear regression analysis of the last four ($I$ and $t$) data points. The calculations performed with this criterion were denoted as $i_{sR}$, $b_{sR}$, $\beta_R$ and $\gamma_R$. This algorithm was used by Yilmaz et al. (2023) to obtain a reference $i_s$ value but it was not directly considered for parameterizing the Haverkamp infiltration model.

Another estimate of the four parameters, denoted as $i_{sT}$, $b_{sT}$, $\beta_T$ and $\gamma_T$, was obtained in accordance with the algorithm used by Yilmaz et al. (2023) and Di Prima et al. (2021) and pioneered by Bagarello, Iovino, and Reynolds (1999). This algorithm considers the last four points of the infiltration curve and then performs a linear regression to calculate the slope, which is regarded as the reference slope, denoted $i_{sR}$. The program then increments the number of points considered for the linear regression by one and computes the slope for this new dataset, involving the $k$ last points and denoted $i_{s(k)}$. Then, the relative error between the new slope, $i_{s(k)}$, and the reference slope, $i_{sR}$, is computed:

$$E_r(k) = \frac{i_s(k) - i_{sR}}{i_{sR}} \tag{9}$$

The number of data points, $k$, is increased until the relative error exceeds a given threshold, fixed arbitrarily at 0.005, as in Yilmaz et al. (2023). The final number of data points, $k$, is used to define the portion of the cumulative infiltration corresponding to the steady state. This method is referred to as the T-algorithm. The advantage of this algorithm, which involves more points than the initial method, is evident for experimental data with measurement errors. Adding points helps capture the overall trend and reduces the risk of misestimations related to the selection of specific or inappropriate points.

The original outputs of the numerical simulations were considered to apply the R- and T-algorithms.

Working with too many infiltration data points may be impractical and, in field use of the Beerkan method (Braud et al. 2005; Lassabatère et al. 2006) the time interval between two subsequent readings may not be very short as it is necessary to wait for the complete infiltration of a pre-established volume of water before pouring another water volume. Therefore, $i_s$ and $b_s$ were also obtained by linear regression of the last four ($I$ and $t$) data points of the resampled cumulative infiltrations and the calculations performed with this algorithm (RR-algorithm; R = reference; R = resampled infiltration data) were denoted as $i_{sRR}$, $b_{sRR}$, $\beta_{RR}$ and $\gamma_{RR}$.

The effect of the used algorithm on estimation of time to steady-state, $t_{steady}$, was initially checked by comparing the cumulative frequency distributions of the ratio between $t_{steady}$ and the duration of the simulation, $t_{sim}$, for the three algorithms. This comparison was made because estimated equilibration times can be expected to change with the applied data analysis method (Bagarello, Iovino, and Reynolds 1999).

A comparison was established between the R- and T-algorithms to verify, for a given sequence of data points describing a cumulative infiltration curve, the impact of the applied steady-state attainment algorithm on the estimates of $i_s$, $b_s$, $\beta$ and $\gamma$.

**TABLE 2** | Initial saturation degree, $S_{ei}$, ratio between the initial ($\theta_i$) and the saturated ($\theta_s$) volumetric soil water content, ratio between the initial ($K_i$) and the saturated ($K_s$) soil hydraulic conductivity, theoretical value of the soil sorptivity ($S$; Yilmaz et al. 2023), slope of the straight line fitted to the data describing steady-state infiltration on the cumulative infiltration vs. time plot ($i_s$), corresponding value of the intercept ($b_s$) and optimised $\beta$ and $\gamma$ values for different soils and initial saturation degrees, $S_{ei}$ ($i_{sT}$, $b_{sT}$, $\beta_T$ and $\gamma_T$ = values obtained by the T-criterion for flow steadiness; $i_{sR}$, $b_{sR}$, $\beta_R$ and $\gamma_R$ = values obtained by the R-criterion; $i_{sRR}$, $b_{sRR}$, $\beta_{RR}$ and $\gamma_{RR}$ = values obtained by applying the RR-criterion).

| Soil | $S_{ei}$ | $\theta_i/\theta_s$ | $K_i/K_s$ | $S$ (mm/h$^{0.5}$) | $i_{sT}$ (mm/h) | $b_{sT}$ (mm) | $i_{sR}$ (mm/h) | $b_{sR}$ (mm) | $i_{sRR}$ (mm/h) | $b_{sRR}$ (mm) | $\beta_T$ | $\gamma_T$ | $\beta_R$ | $\gamma_R$ | $\beta_{RR}$ | $\gamma_{RR}$ |
|---|---|---|---|---|---|---|---|---|---|---|---|---|---|---|---|---|
| Sand (Sa) | 0.05 | 0.149 | $6.23\times10^{-6}$ | 88.92 | 718.9 | 13.2 | 717.2 | 13.9 | 717.4 | 13.8 | 1.018 | 0.976 | 0.912 | 0.972 | 0.926 | 0.972 |
| | 0.1 | 0.194 | $8.09\times10^{-5}$ | 86.44 | 718.4 | 12.5 | 716.0 | 13.6 | 717.1 | 13.1 | 1.011 | 0.977 | 0.855 | 0.972 | 0.927 | 0.974 |
| | 0.2 | 0.284 | $1.07\times10^{-3}$ | 81.26 | 718.1 | 10.9 | 716.4 | 11.6 | 716.8 | 11.4 | 1.041 | 0.982 | 0.915 | 0.978 | 0.945 | 0.979 |
| | 0.3 | 0.373 | $4.90\times10^{-3}$ | 75.68 | 717.7 | 9.34 | 716.4 | 9.85 | 716.5 | 9.81 | 1.076 | 0.990 | 0.968 | 0.987 | 0.975 | 0.987 |
| Loamy-sand (LoSa) | 0.05 | 0.182 | $1.64\times10^{-6}$ | 59.88 | 336.4 | 13.78 | 335.5 | 14.5 | 335.3 | 14.7 | 0.791 | 0.891 | 0.713 | 0.887 | 0.694 | 0.886 |
| | 0.1 | 0.225 | $2.75\times10^{-5}$ | 58.25 | 336.2 | 13.0 | 335.0 | 14.0 | 335.1 | 13.9 | 0.794 | 0.891 | 0.682 | 0.885 | 0.691 | 0.886 |
| | 0.2 | 0.311 | $4.68\times10^{-4}$ | 54.69 | 335.8 | 11.4 | 334.9 | 12.1 | 334.8 | 12.2 | 0.804 | 0.897 | 0.705 | 0.892 | 0.696 | 0.892 |
| | 0.3 | 0.397 | $2.50\times10^{-3}$ | 50.97 | 335.3 | 9.89 | 334.6 | 10.5 | 334.6 | 10.5 | 0.811 | 0.901 | 0.715 | 0.897 | 0.715 | 0.897 |
| | 0.4 | 0.483 | $8.36\times10^{-3}$ | 46.86 | 335.0 | 8.35 | 334.4 | 8.88 | 334.3 | 8.92 | 0.823 | 0.912 | 0.723 | 0.909 | 0.717 | 0.909 |
| Sandy-loam (SaLo) | 0 | 0.159 | 0 | 38.03 | 110.4 | 18.3 | 109.5 | 20.1 | 109.7 | 19.7 | 0.792 | 0.790 | 0.652 | 0.779 | 0.684 | 0.781 |
| | 0.1 | 0.243 | $3.98\times10^{-6}$ | 36.02 | 110.0 | 16.7 | 109.1 | 18.3 | 109.3 | 18.0 | 0.771 | 0.787 | 0.633 | 0.777 | 0.656 | 0.779 |
| | 0.2 | 0.327 | $1.08\times10^{-4}$ | 33.85 | 109.5 | 15.2 | 108.8 | 16.4 | 108.8 | 16.3 | 0.726 | 0.786 | 0.615 | 0.778 | 0.623 | 0.778 |
| | 0.3 | 0.411 | $7.62\times10^{-4}$ | 31.53 | 108.8 | 13.7 | 108.0 | 15.1 | 108.2 | 14.7 | 0.666 | 0.785 | 0.536 | 0.775 | 0.570 | 0.778 |
| | 0.4 | 0.495 | $3.10\times10^{-3}$ | 28.97 | 108.2 | 11.9 | 107.7 | 12.8 | 107.8 | 12.7 | 0.634 | 0.790 | 0.539 | 0.783 | 0.547 | 0.784 |
| Loam (Lo) | 0 | 0.181 | 0 | 22.08 | 31.6 | 19.4 | 31.3 | 20.3 | 31.3 | 20.2 | 1.437 | 0.764 | 1.327 | 0.756 | 1.332 | 0.756 |
| | 0.1 | 0.263 | $1.09\times10^{-7}$ | 20.84 | 31.2 | 18.1 | 30.9 | 19.3 | 31.0 | 18.8 | 1.316 | 0.758 | 1.171 | 0.747 | 1.224 | 0.751 |
| | 0.2 | 0.345 | $7.41\times10^{-6}$ | 19.60 | 30.8 | 16.9 | 30.3 | 18.9 | 30.6 | 17.4 | 1.193 | 0.747 | 0.959 | 0.728 | 1.119 | 0.741 |
| | 0.3 | 0.427 | $8.82\times10^{-5}$ | 18.28 | 30.4 | 15.3 | 30.1 | 16.4 | 30.2 | 15.9 | 1.096 | 0.737 | 0.963 | 0.726 | 1.015 | 0.730 |
| | 0.4 | 0.509 | $5.21\times10^{-4}$ | 16.81 | 30.0 | 13.6 | 29.8 | 14.2 | 29.8 | 14.2 | 0.995 | 0.731 | 0.911 | 0.725 | 0.911 | 0.725 |
| Silty-loam (SiLo) | 0 | 0.149 | 0 | 17.20 | 16.5 | 23.4 | 16.3 | 25.3 | 16.3 | 24.8 | 1.908 | 0.778 | 1.658 | 0.762 | 1.717 | 0.766 |
| | 0.1 | 0.234 | $3.54\times10^{-9}$ | 16.34 | 16.3 | 21.8 | 16.0 | 23.4 | 16.1 | 23.3 | 1.798 | 0.759 | 1.578 | 0.745 | 1.593 | 0.746 |
| | 0.2 | 0.319 | $5.91\times10^{-7}$ | 15.34 | 16.0 | 20.2 | 15.8 | 21.8 | 15.9 | 21.5 | 1.641 | 0.751 | 1.423 | 0.737 | 1.463 | 0.740 |
| | 0.3 | 0.404 | $1.19\times10^{-5}$ | 14.33 | 15.8 | 18.7 | 15.6 | 20.0 | 15.6 | 19.7 | 1.476 | 0.735 | 1.299 | 0.724 | 1.335 | 0.726 |
| | 0.4 | 0.489 | $1.01\times10^{-4}$ | 13.17 | 15.6 | 15.9 | 15.5 | 16.6 | 15.4 | 17.6 | 1.450 | 0.737 | 1.337 | 0.729 | 1.192 | 0.721 |

(Continues)

**TABLE 2** | (Continued)

| Soil | $S_{ei}$ | $\theta_i/\theta_s$ | $K_i/K_s$ | $S$ (mm/h$^{0.5}$) | $i_{sT}$ (mm/h) | $b_{sT}$ (mm) | $i_{sR}$ (mm/h) | $b_{sR}$ (mm) | $i_{sRR}$ (mm/h) | $b_{sRR}$ (mm) | $\beta_T$ | $\gamma_T$ | $\beta_R$ | $\gamma_R$ | $\beta_{RR}$ | $\gamma_{RR}$ |
|---|---|---|---|---|---|---|---|---|---|---|---|---|---|---|---|---|
| Silt (Si) | 0 | 0.074 | 0 | 14.25 | 10.2 | 25.1 | 9.93 | 27.8 | 10.1 | 26.1 | 2.450 | 0.803 | 2.049 | 0.779 | 2.284 | 0.794 |
| | 0.1 | 0.167 | $9.07\times10^{-10}$ | 13.56 | 9.99 | 23.3 | 9.70 | 26.7 | 9.90 | 24.4 | 2.340 | 0.782 | 1.832 | 0.751 | 2.157 | 0.772 |
| | 0.2 | 0.259 | $2.18\times10^{-7}$ | 12.70 | 9.87 | 21.3 | 9.70 | 23.2 | 9.76 | 22.5 | 2.189 | 0.778 | 1.876 | 0.760 | 1.986 | 0.767 |
| | 0.3 | 0.352 | $5.41\times10^{-6}$ | 11.85 | 9.71 | 19.4 | 9.63 | 20.3 | 9.61 | 20.5 | 2.006 | 0.765 | 1.850 | 0.756 | 1.819 | 0.755 |
| | 0.4 | 0.444 | $5.34\times10^{-5}$ | 10.92 | 9.53 | 17.4 | 9.40 | 19.0 | 9.42 | 18.7 | 1.817 | 0.754 | 1.550 | 0.739 | 1.599 | 0.742 |

Another comparison was carried out between the R- and RR-algorithms to verify, for a given number of data points used for the regression, the dependence of the estimated $i_s$, $b_s$, $\beta$ and $\gamma$ values on the duration of the time interval between two subsequent data points.

Following Yilmaz et al. (2023), representative values of $\beta$ and $\gamma$ for each soil in the $0.1 \le S_{ei} \le 0.3$ range of values were then calculated by averaging the results obtained with the T-, R- and RR-algorithms.

Finally, the accuracy of the $S$ and $K_s$ predictions was determined using BEST-steady by considering (i) the default values of $\beta$ and $\gamma$ (0.6 and 0.75, respectively), (ii) the soil-dependent $\beta$ and $\gamma$ values suggested by Yilmaz et al. (2023) and (iii) the soil-dependent $\beta$ and $\gamma$ values obtained in this investigation with the RR-algorithm, which is considered to be the best one (as discussed in the Results section). The $i_{sRR}$ and $b_{sRR}$ estimates were used for these calculations since they were considered to be those conceptually closest to the values that can be obtained with a field experiment. Moreover, $K_i = 0$ was assumed in Equation (4), as is done in practical application of the method. According to Reynolds (2011), an estimated value was considered accurate when the following condition was satisfied:

$$0.8 \le \frac{\text{estimated value}}{\text{theoretical value}} \le 1.2 \tag{10}$$

Such an accuracy criterion (i.e., $\le 20\%$ error) was used because the data were numerically generated and therefore devoid of measurement error and natural variability. The applied criterion was a little more restrictive than the one later applied by the same author in another investigation with numerically simulated data, in which the estimates were considered accurate if the error did not exceed the 25% (Reynolds 2013). The choice of the accuracy criterion has unavoidably a subjective character and a 20% error could be considered large. In this investigation it was preferred not to deviate from other investigations rather than suggesting other error levels.

## 3 | Results

### 3.1 | Steady-State Attainment Algorithm

The three applied algorithms (T, R and RR) differed appreciably with reference to the estimated time to steady-state, $t_{steady}$ (Figure 2). In particular, the T-algorithm provided the earliest stabilisation prediction ($0.25 \le t_{steady}/t_{sim} \le 0.78$; mean = 0.55) whilst the most delayed one was obtained with the R-algorithm ($0.92 \le t_{steady}/t_{sim} \le 0.99$; mean = 0.98). The RR-algorithm yielded an intermediate result ($0.75 \le t_{steady}/t_{sim} \le 0.92$; mean = 0.85), that was however closer to that obtained with the R-algorithm than the T-one. Therefore, the process was considered stable only in the last minutes of the run with the R-algorithm, for a little longer period with the RR-algorithm and for an appreciably longer period with the T-algorithm.

The T-algorithm yielded higher $i_s$ values (Figure 3a,b) and smaller $b_s$ values (Figure 3c,d) than the R-algorithm for the $N = 29$ simulated infiltration runs (Table 2). In particular, $i_{sT}$

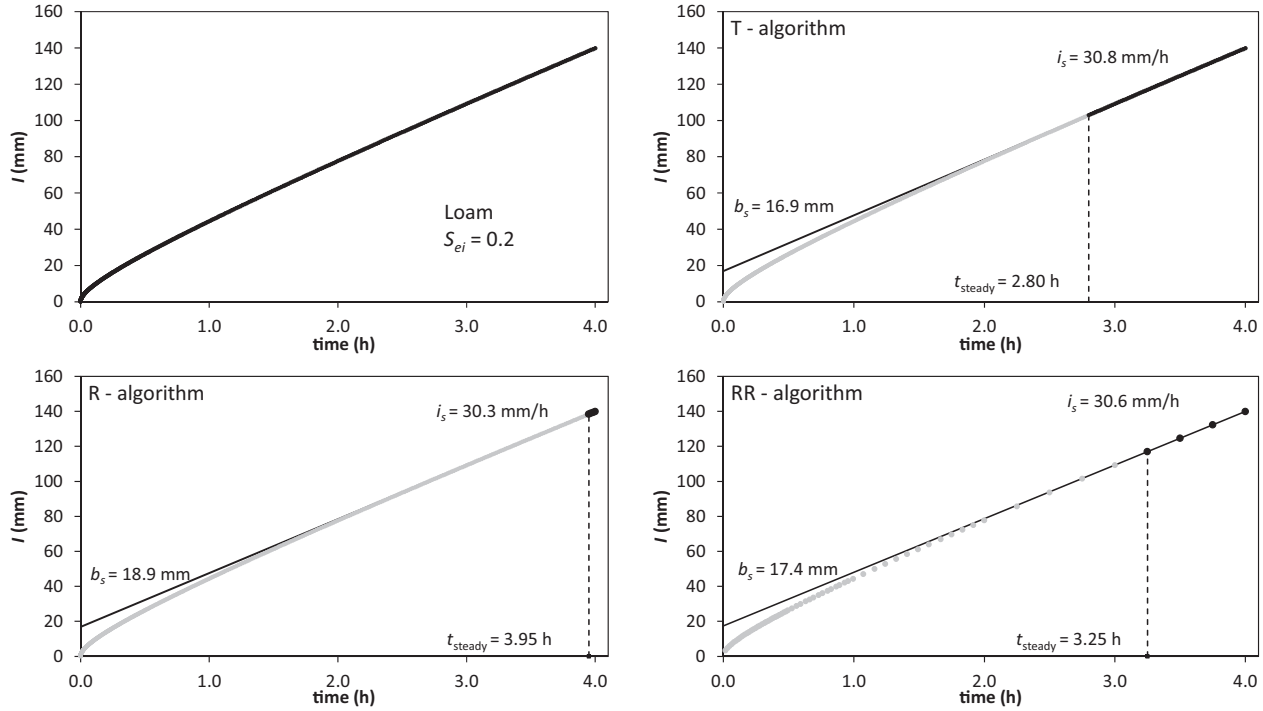


**FIGURE 1** | Example of application of the T-, R- and RR-algorithms for the loam soil with an initial saturation degree, $S_{ei}=0.2$ ($t_{steady}$ = time to steady-state; $i_s$ and $b_s$ = slope and intercept, respectively, of the straight line fitted to the data describing steady-state conditions).

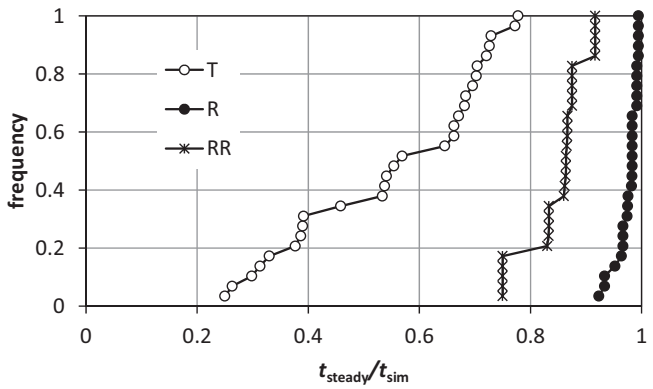


**FIGURE 2** | Cumulative empirical frequency distribution of the ratio between the estimated time to steady-state, $t_{steady}$, and the duration of the simulation, $t_{sim}$, for the T-, R- and RR-algorithms.

was greater than $i_{sR}$ by a percentage, $\Delta i_s$, varying with the run between 0.2% and 3.0% and equal, on average, to 0.9%. Instead, $b_{sT}$ was smaller than $b_{sR}$ by a percentage, $\Delta b_s$, varying with the run from −12.8% to −4.1% and equal, on average, to −7.0%. Therefore, the applied steady-state attainment algorithm influenced the $i_s$ and $b_s$ calculations but, in percentage terms, $i_s$ was appreciably less sensitive to the applied algorithm than $b_s$. These trends result from the fact that the T-algorithm is less discriminating than the R-algorithm to select steady-state and includes a larger time interval.

The mean of $\Delta i_s$ was equal to 1.9% for the Si soil and ≤1.2% for the other five soils. The mean of $\Delta b_s$ was equal to −8.7% for the Si soil and ≥−8.3% in the other cases. Therefore, the finest soil investigated in this study, that is, silt, was the most sensitive to the applied steady-state attainment algorithm.

To establish if the effects of the applied algorithm varied with $S_{ei}$, the results obtained for the two coarsest soils with $S_{ei}=0.05$ and those obtained for the other soils with $S_{ei}=0$ were pooled together and we then compared results between groups of initial saturation degrees. The means of $\Delta i_s$ settled on a value of 1.0%–1.1% for $S_{ei}\leq 0.2$ and to 0.7% for $S_{ei}\geq 0.3$. The mean of $\Delta b_s$ varied between −6.0% and −6.3% for $S_{ei}\geq 0.3$ and it was a little more negative (from −6.7% to −8.2%) in initially drier conditions ($S_{ei}\leq 0.2$). Therefore, the effect of the steady-state attainment algorithm appeared overall a little more appreciable in relatively dry initial conditions.

The $\beta$ and $\gamma$ values obtained with the T-algorithm were greater than those obtained with the R-algorithm (Figure 4 and Table 2). In particular, the percentage difference between $\beta_T$ and $\beta_R$, $\Delta\beta$, varied from a minimum of 8.3% to a maximum of 27.7% with a mean of 15.6%. The percentage difference between $\gamma_T$ and $\gamma_R$, $\Delta\gamma$, varied from a minimum of 0.3% to a maximum of 4.0% with a mean of 1.3%. Therefore, the applied steady-state attainment algorithm (T- or R-algorithm) influenced the calculations of $\beta$ and $\gamma$ but, in percentage terms, $\gamma$ was appreciably less sensitive to the applied algorithm than $\beta$. This last result was expected since $\gamma$ depends on $i_s$ through Equation (5) whereas $\beta$ depends on $b_s$ through Equation (6) and $i_s$ varied with the applied steady-state algorithm less than $b_s$ (Figure 3).

### 3.2 | Effect of Storing Time Step of the Numerically Simulated Infiltration Data

In this section, we compare the two algorithms that define steady-state based on the four last points. The R-algorithm considers the four last points of the raw numerical dataset with

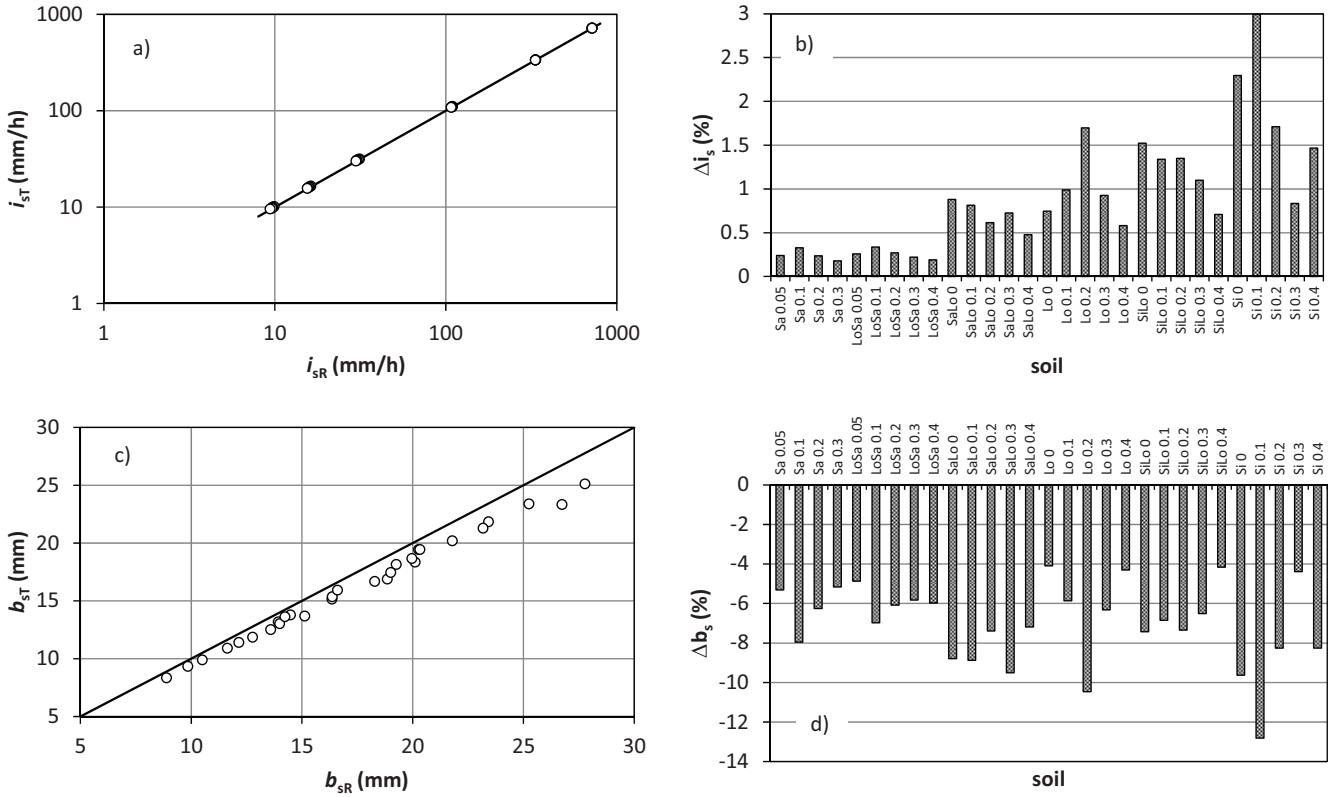


**FIGURE 3** | Comparison between (a) the slope, $i_s$, and (c) the intercept, $b_s$, of the straight line fitted to the cumulative infiltration data describing steady-state conditions obtained by the T-algorithm (T = threshold; $i_{sT}$ and $b_{sT}$) and the R-algorithm (R = reference; $i_{sR}$ and $b_{sR}$), and percentage differences between corresponding (b) $i_s$ ($\Delta i_s$) and (d) $b_s$ ($\Delta b_s$) values for each soil and initial saturation degree.

time steps between two readings of ≤1 min. In a closer accordance with real experimental protocols, the second algorithm considers time steps of ≤15 min. With a few exceptions, the RR-algorithm yielded higher $i_s$ values (Figure 5a,b) and smaller $b_s$ values (Figure 5c,d) than the R-algorithm for the $N = 29$ simulated infiltration runs (Table 2). In particular, $i_{sRR}$ differed from $i_{sR}$ by a percentage, $\Delta i_s$, varying with the run between −0.8% and 2.0% and equal, on average, to 0.2%. Instead, $b_{sRR}$ differed from $b_{sR}$ by a percentage, $\Delta b_s$, varying with the run from −8.7% to 6.2% and equal, on average, to −1.5%. Therefore, the storing time step of the numerically simulated infiltration data influenced calculation of $i_s$ and $b_s$. In percentage terms, $i_s$ was appreciably less sensitive to the considered time step than $b_s$. However, the discrepancy between the RR and R-algorithms was much less than before. Indeed, the two algorithms are quite close to each other and select quite similar time intervals, compared to the much larger interval identified by the T-algorithm.

The mean of $\Delta i_s$ was equal to 0.8% for the Si soil and it varied from nearly zero (−0.01%) to 0.4% for the other five soils. The mean of $\Delta b_s$ was equal to −3.7% for the Si soil and it varied from −2.5% to 0.3% in the other cases. Therefore, the finest soil was also the most sensitive soil to the considered storing time step.

The means of $\Delta i_s$ settled on a value of 0.3%–0.5% for $S_{ei} \leq 0.2$ and to values ranging from −0.1% to 0.1% for $S_{ei} \geq 0.3$. The mean of $\Delta b_s$ varied between −2.9% and −1.6% for $S_{ei} \leq 0.2$ and from −1.0% to 0.8% for $S_{ei} \geq 0.3$. Therefore, the effect of the storing time step was a little more appreciable in initially drier soil conditions. We find similar results as before. The dry initial conditions and the type of soil defined as silty soil accentuate the difference between criteria.

The $\beta$ and $\gamma$ values obtained with the RR-algorithm were generally greater than those obtained with the R-algorithm (Figure 6 and Table 2). In particular, the percentage difference between $\beta_R$ and $\beta_{RR}$, $\Delta\beta$, varied from a minimum of −10.9% to a maximum of 17.7% with a mean of 3.2%. The percentage difference between $\gamma_R$ and $\gamma_{RR}$, $\Delta\gamma$, varied from a minimum of −1.2% to a maximum of 2.7% with a mean of 0.3%. Therefore, the considered time to acquire data (R- or RR-algorithms) influenced the calculations of $\beta$ and $\gamma$ but, also in this case, $\gamma$ was less sensitive to the applied algorithm than $\beta$. Even this result was expected since $i_s$ varied with the storing time less than $b_s$ (Figure 5). Note that our results are in line with previous findings and demonstrate the effect of inappropriate selection of steady-state on the computation of the shape parameters $\beta$ and $\gamma$.

### 3.3 | Soil Dependent $\beta$ and $\gamma$ Parameters

According to Yilmaz et al. (2023), utterly dry conditions, such as an initial saturation degree below 0.1, are rarely observed during field experiments. Moreover, infiltration runs can also be performed in wetter, but not much wetter, initial conditions, ensuring that $S_{ei} \leq 0.3$. Note that the value of 0.3 is also in line with the condition imposed by Haverkamp et al. (1994) for the use of their analytical model and related approximate expansions, which serve as the basis for many treatment methods and algorithms, including the BEST methods (Angulo-Jaramillo

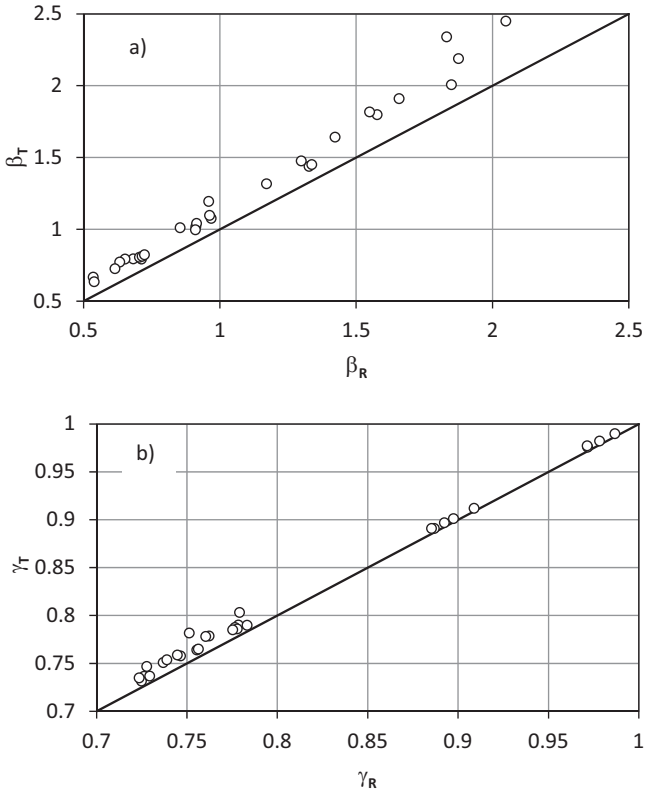


**FIGURE 4** | Comparison between the estimates of (a) the $\beta$ parameter and (b) the $\gamma$ parameter obtained by estimating the steady-state conditions with the T-algorithm (T = threshold; $\beta_T$ and $\gamma_T$) and the R-algorithm (R = reference; $\beta_R$ and $\gamma_R$).

et al. 2019). Given this premise, and also considering that, in this investigation, the $0.1 \leq S_{ei} \leq 0.3$ range was common to the six soils, the means of the three estimates of both $\beta$ ($\beta_T$, $\beta_R$ and $\beta_{RR}$) and $\gamma$ ($\gamma_T$, $\gamma_R$ and $\gamma_{RR}$) were calculated for each soil with reference to this range of antecedent wetness conditions (Table 3). Evidently, the means of $\beta_T$ and $\gamma_T$ listed in Table 3 coincided with those calculated using the $\beta$ and $\gamma$ values reported by Yilmaz et al. (2023) in their Table 2 since the same data and the same procedure were applied.

For a given soil (Sa, LoSa, SaLo, Lo, SiLo and Si) and a given algorithm (T, R and RR), the coefficient of variation, *CV*, of the three estimates of $\beta$ (one for each $S_{ei}$ value in the 0.1 to 0.3 range) varied from a minimum of 1.1% ($\beta_T$, LoSa soil) to a maximum of 11.8% ($\beta_R$, Lo soil) with a mean of 6.5%. For $\gamma$, the *CV* values varied from 0.1% ($\gamma_{RR}$, SaLo soil) to 1.6% ($\gamma_T$, SiLo soil) with a mean of 0.9%. Therefore, $\gamma$ varied less than $\beta$ with $S_{ei}$ but both parameters were quite stable in the $0.1 \leq S_{ei} \leq 0.3$ range of values.

The means of $\beta$, obtained by averaging the three estimates of $\beta$ for a given soil, varied with the soil by 3.1 times. In particular, these means decreased from 0.97 to 0.64 from the Sa soil to the SaLo soil and then they increased up to 2.01 for the Si soil. Therefore, the SaLo soil had the smallest value of $\beta$ whereas both the coarser and, particularly, the finer soils had greater $\beta$ values. The analysis algorithm of the numerically simulated infiltration data influenced the estimates of $\beta$ for a given soil since the ratio between the maximum and the minimum value for a soil varied between 1.14 and 1.21 and the corresponding coefficients of variation, *CV*s, ranged from 6.9% to 10.5%, depending on the soil. A *CV* value that does not exceed, in practise, the 10% can be considered indicative of an overall limited variability of the individual data (Warrick 1998). Therefore, the calculated means appeared sufficiently reliable for most practical purposes.

Another point arises from the values of $\beta$. All soils exhibit a value of $\beta$ greater than one, with silt soils having $\beta$ values exceeding 2 (Table 3, Si soil). Similar results were obtained by Yilmaz et al. (2023) for fine soils (see Table 2 in Yilmaz et al. 2023). Our findings are also consistent with previous studies using numerically generated data for the transient state to derive $\beta$, which found values greater than one and sometimes approaching or exceeding 2 (e.g., Lassabatere et al. 2009; Latorre et al. 2018; Moret-Fernández et al. 2020). Such high values of $\beta$ raise questions regarding the physical meaning and the analytical developments proposed by Haverkamp et al. (1994) for their infiltration model. Haverkamp et al. (1994) suggested that $\beta$ should remain strictly below one to meet the proper conditions for model integration. Lassabatere et al. (2018) demonstrated, using pure analytical data, that the limit of $\beta < 2$ should be respected to maintain consistency with the Haverkamp infiltration model approximations. Whilst the first condition of $\beta < 1$ is not always considered, adhering to the second condition of $\beta < 2$ is essential to prevent inconsistent modelling, which excludes the silt soil and its corresponding $\beta$ value.

The means of $\gamma$, obtained by averaging the three estimates of $\gamma$ for a given soil, varied with the soil by 1.3 times. In this case, however, these means decreased from 0.98 to 0.74 from the Sa soil to the SiLo soil and then they increased only a little, that is to 0.77, for the Si soil. Overall, the coarser soils (Sa and LoSa) had the largest $\gamma$ values (0.89–0.98) whereas the finer soils had smaller $\gamma$ values (0.74–0.78). The analysis algorithm of the numerically simulated data had no more than a minimal, and negligible, effect on the estimates of $\gamma$ for a given soil since the ratio between the maximum and the minimum value for a soil did not exceed 1.03 and the corresponding *CV*s were equal to 1.2% at the most. Therefore, the calculated means appeared reliable in general.

In summary, adopting a soil specific value should be more important for $\beta$ than for $\gamma$ since the former parameter varies with the soil more than the latter one. Using the default value of $\beta$ (0.6) appears a good choice for the SaLo soil and, to a lesser extent, the LoSa soil but not in general, that is regardless of the soil. Instead, the default value of $\gamma$ (0.75) appears usable in many soils, with perhaps the exception of the coarser ones.

### 3.4 | Accuracy of Soil Sorptivity and Saturated Soil Hydraulic Conductivity Estimates

In this section, we evaluated the impact of the choice of the values of $\beta$ and $\gamma$ on the estimates of sorptivity, $S$, and hydraulic conductivity, $K_s$, using the BEST-steady method. We then compared the several sets of values of $S$ and $K_s$ obtained for the regular set of values ($\beta = 0.6$ and $\gamma = 0.75$), and obtained for the T- and RR-algorithms. This latter is considered the best option (as discussed below) and is then taken as the reference. The results of

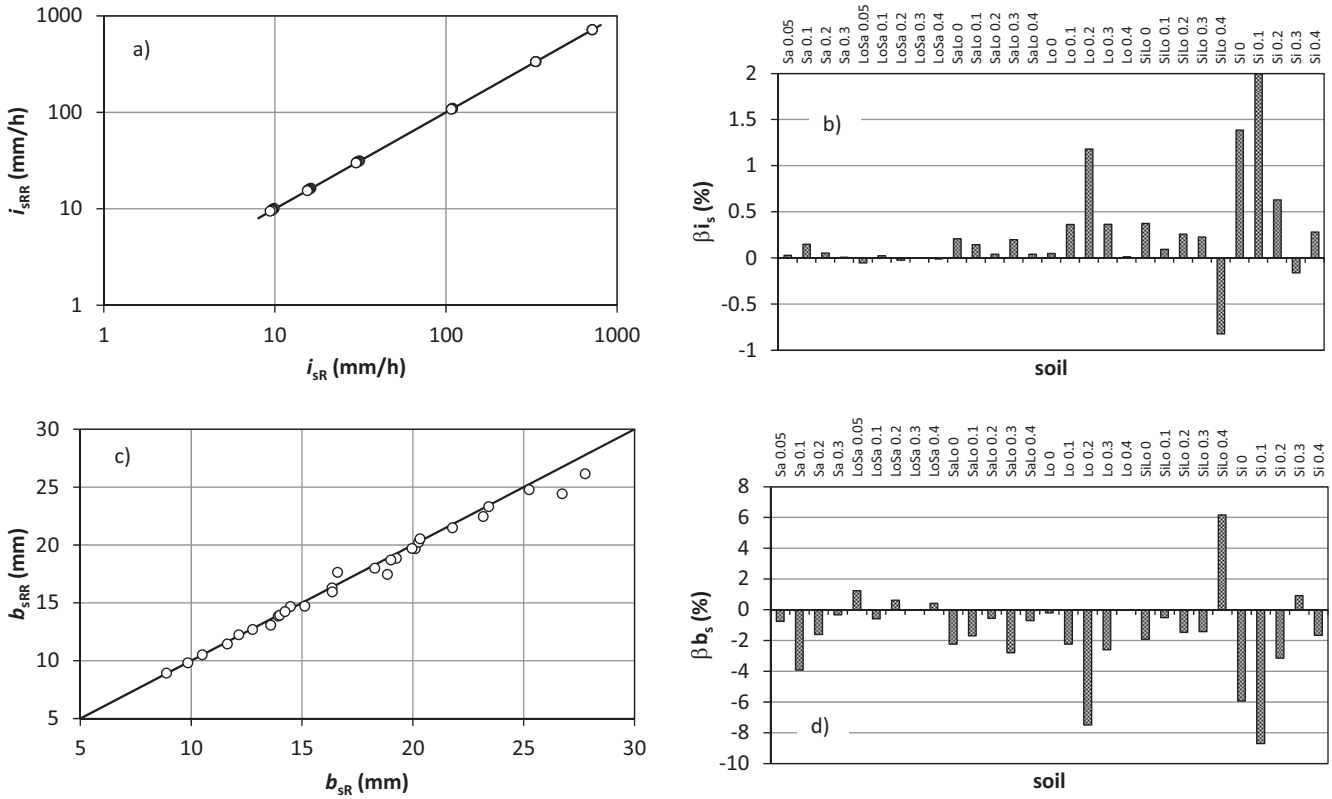


**FIGURE 5** | Comparison between (a) the slope, $i_s$, and (c) the intercept, $b_s$, of the straight line fitted to the cumulative infiltration data describing steady-state conditions obtained by the RR-algorithm (RR = reference, resampled; $i_{sRR}$ and $b_{sRR}$) and the R-algorithm (R = reference; $i_{sR}$ and $b_{sR}$), and percentage differences between corresponding (b) $i_s$ ($\Delta i_s$) and (d) $b_s$ ($\Delta b_s$) values for each soil and initial saturation degree.

the T-algorithm correspond to those of Yilmaz et al. (2023). With reference to the six soils (Sa, LoSa, SaLo, Lo, SiLo and Si), the three $S_{ei}$ values (from 0.1 to 0.3) and the three $\beta$ and $\gamma$ estimating algorithms (T, R and RR), the ratio between the estimated and the theoretical sorptivity fell into a range of values between 0.91 and 1.04 (Figure 7a). Therefore, all estimates of $S$ were accurate according to the adopted criterion (Reynolds 2011). However, in a context of accurate estimates, the three applied criteria to parameterize the Haverkamp et al. (1994) model were not equivalent. In particular, the most accurate predictions were obtained by using $\beta_{RR}$ and $\gamma_{RR}$ since, in this case, the ratio between the estimated and the theoretical $S$ value was consistently very close to 1 in all cases (from 0.99 to 1.01). A minimally greater deviation from the unit value (0.98–1.04) was observed for the ratios between estimated and theoretical values using the T-algorithm. The poorest, but still accurate, predictions of $S$ were obtained using the default values of the two parameters (ratio = 0.91–1.03).

Instead, the ratio between the estimated and the theoretical saturated soil hydraulic conductivity values fell into a range of values between 0.86 and 1.59 (Figure 7b) denoting that not all the $K_s$ predictions were accurate. In particular, the algorithm developed in this investigation performed best and it always yielded accurate predictions ($0.96 \leq$ estimated $K_s$/theoretical $K_s \leq 1.04$). With the $\beta$ and $\gamma$ values by the T-algorithm, the $K_s$ predictions got a little worse, since the range of the ratios between the estimated and the theoretical values became a little wider (0.86–1.18), but they remained accurate. With the default values of $\beta$ and $\gamma$, the ratio between the estimated and the theoretical $K_s$ value varied between 1.01 and 1.59 and the 56% of the predictions were deemed inaccurate according to the adopted accuracy criterion (20% error).

Therefore, this investigation suggested that using the default values of $\beta$ and $\gamma$ should not be expected to compromise the accuracy of the $S$ predictions but there is the risk to overestimate too much $K_s$. The values obtained with the T-algorithm (Yilmaz et al. 2023) are fully appropriate to obtain accurate estimates of both $S$ and $K_s$. The $\beta$ and $\gamma$ values obtained in this investigation can be expected to improve the quality of an already good estimate of these two soil hydrodynamic parameters.

## 4 | Discussion

This investigation showed that the adopted algorithm to analyse the numerically simulated infiltration data (T, R and RR) influenced the estimated parameters. In particular, finer and drier soil conditions implied a more appreciable effect on the estimates of $i_s$ and $b_s$ of both the applied steady-state attainment criterion and the time step at which the data were acquired. Taking into account that the duration of the transient stage of the infiltration process generally increases with finer and drier soil (Youngs, Leeds-Harrison, and Elrick 1995; Reynolds and Elrick 2002; Reynolds, Elrick, and Youngs 2002), the effects of the adopted algorithm were more appreciable as the equilibration time was longer.

The estimates of $b_s$ depended more than those of $i_s$ on the applied algorithm (Figures 3, 5 and Table 2). Consequently, $\beta$

varied more than $\gamma$ amongst the three algorithms (Figures 4, 6 and Tables 2, 3).

It was therefore necessary to establish what algorithm should be preferred in practise, taking into account that they have the same aim, which is defining the steady-state stage of the run in a reliable, objective and hence repeatable way. In practise, however, the duration of the presumed steady-state stage of the process, the amount of infiltrated water during this stage and the number of considered ($I$ and $t$) data points for the regression

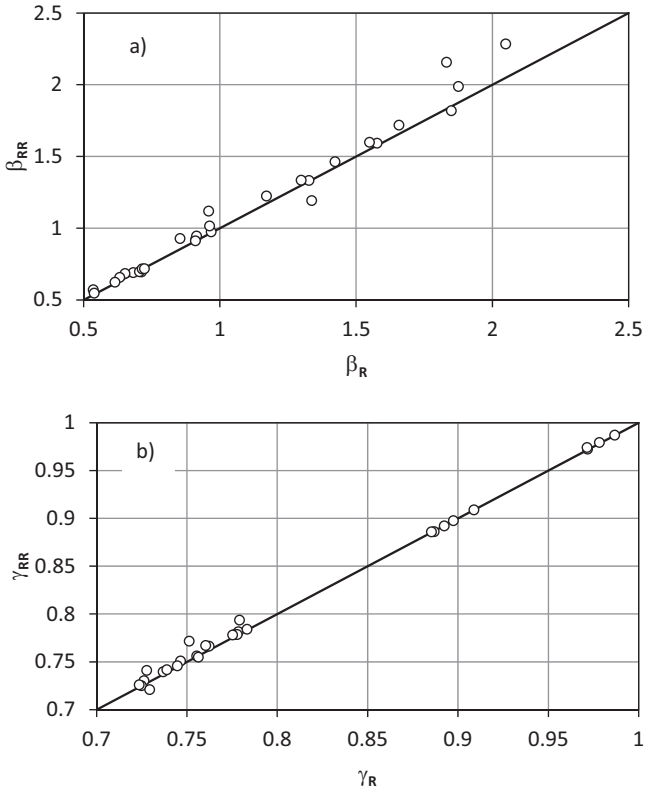


**FIGURE 6** | Comparison between the estimates of (a) the $\beta$ parameter and (b) the $\gamma$ parameter obtained by estimating the steady-state conditions with the RR-algorithm (RR = reference and resampled; $\beta_{RR}$ and $\gamma_{RR}$) and the R-algorithm (R = reference; $\beta_R$ and $\gamma_R$).

can differ greatly with the adopted algorithm, as shown in the two examples (Sa soil, $S_{ei} = 0.05$; and Si soil, $S_{ei} = 0.4$) reported in Table 4. Each algorithm has advantages and disadvantages.

An expected advantage of the T-algorithm is that as many points as possible are considered for linear regression, which in principle assures a good representativeness of the fitted straight line to the data. In particular, data with errors, such as measurement uncertainty in experimental data or numerical dispersion and oscillations in numerical data, may obscure the trend and hinder the characterisation of a steady-state straight line. Increasing the number of data points helps to capture the main trend more accurately. A disadvantage is that the last part of the transient stage of the infiltration process could be considered expressive of the stabilised stage. In this case, $i_s$ will be overestimated and $b_s$ will be underestimated.

The R-algorithm minimises the risk to improperly consider the last part of the transient stage of the infiltration run as expressive of the stabilised stage since the data used for estimating $i_s$ and $b_s$ describe infiltration at the most advanced stage possible. However, the last four data points refer to a short time interval and a small cumulative infiltration amount. Therefore, it can be suspected that any rounding and/or approximation of the data as well as numerical errors due to solving the partial differential equation (numerical dispersion, distortion and oscillations) could have a not negligible effect on the estimates of the two parameters even if the data have been numerically simulated and hence they are free of the perturbations embedded in field and laboratory measurements. Furthermore, an uncertainty on the reference value has to be expected to also affect the estimates of $i_s$ and $b_s$ obtained with the T-algorithm.

The RR-algorithm mediates to some extent between advantages and disadvantages of the T- and R-algorithms, even if it is closer to the R-algorithm than the T-algorithm. The number of data points does not differ as compared with the R-algorithm but, with larger time increments between data points, the steady-state stage considered for the calculations is longer and consequently more water infiltrates. This circumstance suggests a reduced impact of rounding and/or approximation of the data but also a higher risk to include the last part of the transient stage

**TABLE 3** | Soil dependent $\beta$ and $\gamma$ parameters of the Haverkamp et al. (1994) infiltration model for initial saturation degrees ranging from 0.1 to 0.3 obtained with different analysis criteria of the numerically simulated infiltration curves.

| | $\beta$ | | | | | | $\gamma$ | | | | | |
|---|---|---|---|---|---|---|---|---|---|---|---|---|
| **Soil** | $\beta_T$ | $\beta_R$ | $\beta_{RR}$ | **Max/min** | **Mean** | ***CV* (%)** | $\gamma_T$ | $\gamma_R$ | $\gamma_{RR}$ | **Max/min** | **Mean** | ***CV* (%)** |
| Sa | 1.043 | 0.912 | 0.949 | 1.14 | 0.968 | 6.9 | 0.983 | 0.979 | 0.980 | 1.004 | 0.981 | 0.2 |
| LoSa | 0.803 | 0.701 | 0.701 | 1.15 | 0.735 | 8.1 | 0.896 | 0.892 | 0.892 | 1.005 | 0.893 | 0.3 |
| SaLo | 0.721 | 0.595 | 0.617 | 1.21 | 0.644 | 10.5 | 0.786 | 0.777 | 0.778 | 1.012 | 0.780 | 0.6 |
| Lo | 1.202 | 1.031 | 1.119 | 1.17 | 1.117 | 7.7 | 0.747 | 0.734 | 0.741 | 1.018 | 0.740 | 0.9 |
| SiLo | 1.638 | 1.433 | 1.464 | 1.14 | 1.512 | 7.3 | 0.748 | 0.735 | 0.737 | 1.018 | 0.740 | 0.9 |
| Si | 2.178 | 1.852 | 1.987 | 1.18 | 2.006 | 8.2 | 0.775 | 0.756 | 0.764 | 1.025 | 0.765 | 1.2 |

*Note:* $\beta_T$ and $\gamma_T = \beta$ and $\gamma$ values obtained with the T-criterion; $\beta_R$ and $\gamma_R = \beta$ and $\gamma$ values obtained with the R-criterion; $\beta_{RR}$ and $\gamma_{RR} = \beta$ and $\gamma$ values obtained with the RR-criterion.
Abbreviations: *CV* = coefficient of variation; max = maximum; min = minimum.

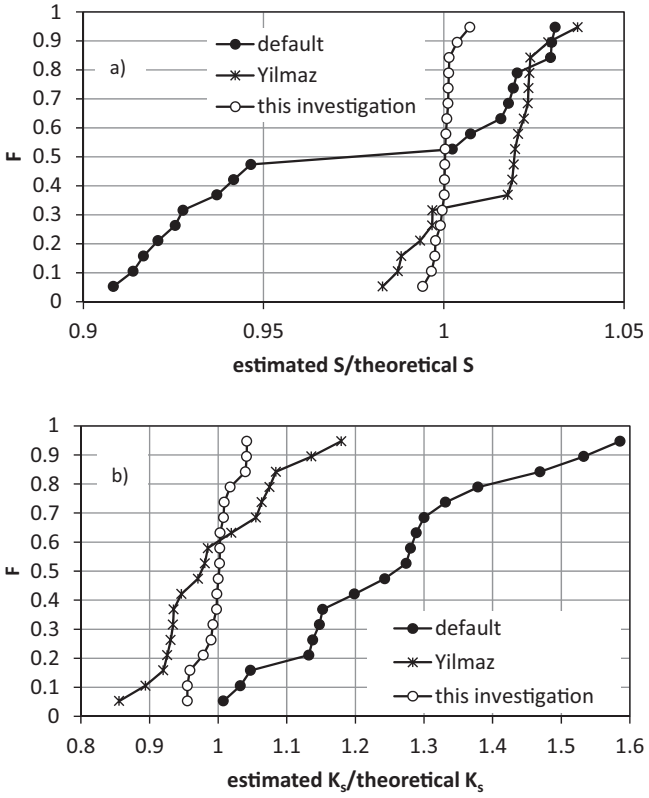


**FIGURE 7** | Cumulative empirical frequency distribution of the ratio between the estimated and true values of (a) soil sorptivity, $S$, and (b) saturated soil hydraulic conductivity, $K_s$ (default: $\beta = 0.6$ and $\gamma = 0.75$; Yilmaz: $\beta$ and $\gamma$ values obtained by Yilmaz et al. (2023) with the T-algorithm; this investigation: $\beta$ and $\gamma$ values obtained for a given soil with the RR-algorithm).

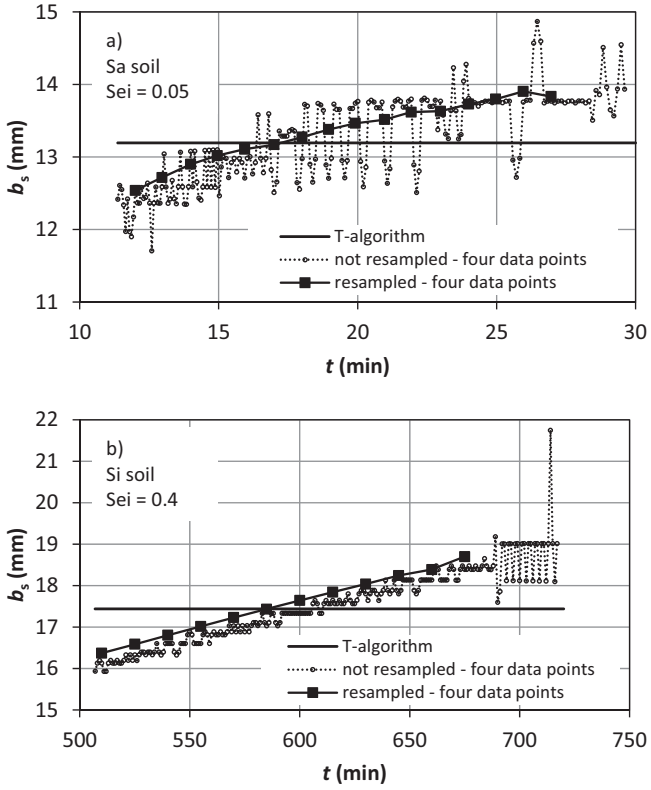


**FIGURE 8** | Comparison between different estimates of the intercept, $b_s$, of the straight line fitted to the cumulative infiltration vs. time, $t$, data during the steady-state stage of the run according to the T-algorithm (T = threshold).

**TABLE 4** | Characteristics of the steady-state stage for two infiltration runs determined with different criteria.

| Infiltration run | Criterion | $\Delta t$ (min) | $\Delta I$ (mm) | DP |
|---|---|---|---|---|
| Sand $S_{ei} = 0.05$ | T | 18.6 | 223.3 | 194 |
| | R | 0.39 | 4.6 | 4 |
| | RR | 3.0 | 36.3 | 4 |
| Silt $S_{ei} = 0.4$ | T | 213.0 | 33.7 | 214 |
| | R | 3.0 | 0.47 | 4 |
| | RR | 45.0 | 7.1 | 4 |

*Note:* $\Delta t$ = final ($t_f$; end of the run) – initial ($t_i$) time of the considered steady-state stage; $\Delta I$ = difference between the cumulative infiltration at $t = t_f$ and $t = t_i$; DP = number of considered data points for the regression.
Abbreviations: R = reference; RR = resampled and reference; T = threshold.

in the calculations. Zhang et al. (2017) also concluded that, at least in the field, a relatively long time-step length avoids short-time measurement errors and reduces operational difficulties.

According to this investigation, the algorithm to be preferred is the one yielding the most convincing estimates of $b_s$ and hence $\beta$ since these two parameters showed a clear dependence on the applied algorithm whilst the dependence of $i_s$ and $\gamma$ was minimal.

As an example for the same runs considered in Table 4, Figure 8 shows, with reference to the steady-state stage of the process estimated by the T-algorithm, the single $b_s$ value obtained with this algorithm and the intercepts calculated for all possible quatrains of ($I$ and $t$) data. To be clearer, the first estimate of $b_s$ in the figure was obtained by considering the first four ($I$ and $t$) data points falling in the steady-state stage of the run. The second pair was obtained by excluding the first ($I$ and $t$) data point from the quatrain and including the fifth ($I$ and $t$) data point. And so on until the last quatrain that included the last four ($I$ and $t$) pairs. This analysis was made by quatrains since this was the sample size previously considered (Yilmaz et al. 2023) to calculate the reference slope. Calculations of $b_s$ by quatrains were made for both the original output simulations (raw numerical data) and the resampled data. The estimates of $b_s$ obtained with the T-algorithm were smaller than those obtained with the other two algorithms by the end of the run. This result reinforced the suspect that, with the T-algorithm, calculation of $b_s$ can be expected to be biased due to the presence, in the considered dataset, of the last part of the transient stage of the infiltration run. The estimates of $b_s$ obtained with the R-algorithm tended to stabilise by the end of the run but they were rather noisy. It was enough to substitute a single data point in the quatrain to obtain an appreciably different estimate of $b_s$. This circumstance raised some doubt about the degree of representativeness of the last quatrain of data for defining a reference slope and hence a reference intercept. In other words, it was not possible to state that this last data point was not influenced by the detected noise. The noise in the $b_s$ values appeared less significant with the RR-algorithm,

confirming that it was preferable to the other two algorithms. In other words, although the RR-algorithm does not guarantee perfect estimates, it probably makes the impacts of the predictable uncertainties with the other two algorithms less relevant.

Regardless of the applied algorithm, $\beta$ and $\gamma$ were calculated by assuming that each run reached steady-state. Plotting $b_s$ against time can help to establish if the run has really stabilised. Regardless of the noise, a nearly horizontal $b_s$ vs. $t$ relationship (e.g., Figure 8a) suggests that steady-state conditions were achieved since, in this case, this intercept has to become constant if two groups of data are extracted from the steady-state stage of the run. A $b_s$ vs. $t$ relationship that ends by still signalling a positive slope (e.g., Figure 8b) does not prove that steadiness was not reached since the last ($b_s$ and $t$) data point could actually represent the first point of the nearly stabilised stage. However, it suggests the opportunity to support this hypothesis by performing longer simulations. A similar approach, that is testing presumably steady flow rates against flow rates at very long times, was followed in other investigations making use of numerically simulated data (Kindred and Reynolds 2020).

In some previous investigations it was suggested that approximations in $\beta$ and $\gamma$ should have a limited effect on prediction of soil sorptivity and saturated soil hydraulic conductivity (Nasta et al. 2012; Moret-Fernández et al. 2020; Rahmati et al. 2020). According to this investigation, a distinction has to be made between $S$ and $K_s$. Approximations in $\beta$ and $\gamma$ actually have negligible effects with reference to prediction of $S$ but they may yield unacceptable results regarding the estimate of $K_s$. Both Yilmaz et al. (2023) and this investigation provide $\beta$ and $\gamma$ values yielding very accurate estimates of the two soil hydrodynamic parameters with BEST-steady (Bagarello, Di Prima, and Iovino 2014). In both cases, knowledge of soil textural characteristics is enough to choose appropriate values for the calculations. Therefore, in future applications of BEST-steady, it is recommended to use these new values of $\beta$ and $\gamma$ with the confidence of expecting, at least in ideal conditions, accurate estimates of both $S$ and $K_s$.

Two points that overall emerge from this and other investigations (Lassabatere et al. 2009; Moret-Fernández and Latorre 2017; Latorre et al. 2018; Moret-Fernández et al. 2020; Rahmati et al. 2020; Yilmaz et al. 2023) are that: (i) $\beta$ cannot be considered a constant since it is a soil dependent parameter; and (ii) the estimate of $b_s$ is more uncertain than that of $i_s$. These results can be expected to have several implications, two of which are briefly discussed in the following.

According to Di Prima et al. (2020) and Yilmaz (2021), the macroscopic capillary length, $\lambda_c$ (L) (White and Sully 1987), used in many simplified calculation methods of $K_s$ (Reynolds and Elrick 1990; Bagarello, Iovino, and Elrick 2004; Bagarello et al. 2014; Bagarello, Di Prima, and Iovino 2017; Nimmo et al. 2009; Stewart and Abou Najm 2018), can be obtained from a beerkan run reaching steady-state by the following relationship:

$$\lambda_c = \frac{b}{\frac{1}{2(1-\beta)}\ln\left(\frac{1}{\beta}\right)} \frac{b_s}{\theta_s - \theta_i} \tag{11}$$

in which $b$ can be set equal to 0.55. Both Di Prima et al. (2020) and Yilmaz (2021) also suggested the following more concise form of Equation (11), obtained by assuming that $\beta$ can be set equal to 0.6:

$$\lambda_c = 0.861 \frac{b_s}{\theta_s - \theta_i} \tag{12}$$

Taking into account that $\beta = 0.6$ does not represent a good choice for many soils, Equation (12) cannot be recommended for a general use. Instead, $\lambda_c$ should be estimated by Equation (11), with the appropriate $\beta$ value for the tested soil (Table 3).

For a 3D infiltration run reaching steadiness, $K_s$ can be estimated from both $b_s$ and $i_s$ or only from $i_s$. Both parameters have to be considered if $K_s$ is obtained by Equation (2), that is to say with BEST-steady (Bagarello, Di Prima, and Iovino 2014). Only $i_s$ is enough if, for example, the purely steady-state method by Reynolds and Elrick (1990) is applied. According to this investigation, using only $i_s$ could be considered the best choice for obtaining accurate estimates of $K_s$ given that $b_s$ appears a more uncertain parameter. However, the reasoning to be done is more complex since, with a purely steady-state method, there is one equation with two unknowns. Therefore, obtaining $K_s$ requires either assuming that the ratio between the two unknowns is known or applying an appropriate experimental methodology, such as the two-ponding-depth approach for the single-ring infiltrometer (Reynolds and Elrick 1990). Therefore, even a purely steady-state approach cannot be considered free from uncertainties. In other words, establishing differences between the estimates of $K_s$ obtained with the two mentioned approaches (from both $b_s$ and $i_s$ or only from $i_s$) seems a practically relevant scientific topic needing consideration.

Finally, this investigation and that by Yilmaz et al. (2023) were performed with reference to a single ring radius ($r = 50$ mm). The estimates of $\beta$ and $\gamma$ could be considered of general validity since these parameters only depend on initial and saturated soil water content and the hydraulic conductivity and diffusivity functions (Fuentes et al. 1998; Lassabatere et al. 2009). However, considering other ring radii could be advisable to verify if the expected correspondence between theory and numerical experiments is actually detectable. Another reason why these additional simulations should be made is that, according to Haverkamp et al. (1994), for increasing radius but identical initial and boundary conditions, the value of $\gamma$ increases slightly.

## 5 | Conclusions

The applied algorithm to select the steady-state stage of a 3D numerically simulated infiltration curve can be expected not to influence very much estimation of the $\gamma$ parameter of the Haverkamp infiltration model but it also has a rather appreciable impact on estimation of the $\beta$ parameter. The reason is that the slope, $i_s$, of the straight line fitted to the data selected for describing steady-state conditions on the cumulative infiltration plot is more stable than the corresponding intercept, $b_s$, that is therefore a more unstable and uncertain parameter.

None of the algorithms tested in this investigation is free from uncertainties and approximations but, amongst these

algorithms, the one that seems most convincing, representing a good compromise between advantages and disadvantages of the other algorithms, is the algorithm named RR. With this criterion, the simulated infiltration curve is initially resampled at fixed and practical time intervals and then $i_s$ and $b_s$ are obtained by linear regression analysis of the last few data points. These data satisfy the condition of maximum representativeness of the stabilised stage of the infiltration run and simultaneously they refer to time intervals and cumulative infiltration amounts large enough to reduce the risk of estimates of $i_s$ and $b_s$ being affected by rounding and approximations or even errors in the data.

The doubts about the reliability of the estimates of $b_s$ can be reduced if this parameter is calculated for all possible groups of data that define a cumulative infiltration curve.

It was confirmed that the $\beta$ and $\gamma$ parameters depend on the soil since, in this investigation, they were found to vary in the 0.62–1.99 and 0.74–0.98 ranges, respectively. In the perspective to use the Haverkamp model for determining soil hydrodynamic properties, the choice of these two parameters amongst different possible alternatives has a limited and practically negligible impact regarding soil sorptivity, $S$, but it could lead to inaccurate predictions of saturated soil hydraulic conductivity, $K_s$. Therefore, it is recommended to generally use soil dependent parameters for the calculations of $S$ and $K_s$.

The results obtained in this investigation can be expected to have an impact in practise, given that the T- and RR-algorithms are two possible options for the analysis of a Beerkan run in the field, and in other contexts such as estimation of the macroscopic capillary length by a Beerkan run or the choice of the experimental methodology to be applied in the field for determining $K_s$ by a single-ring infiltration technique.

This investigation was performed by considering a single ring radius and infiltration runs of long but pre-fixed duration. It is therefore advisable to verify if the results are confirmed in other contexts including other ring radii and other criteria to establish that steadiness has been reached by the end of the run. It should also be verified if the $\beta$ and $\gamma$ values obtained in this investigation apply in general to the available BEST algorithms.

This investigation could contribute to an improved description of the soil hydrodynamic properties, and hence the soil hydrological processes, in relevant contexts with reference to soil erosion processes and their impact on the environment.

## Data Availability Statement

The data that support the findings of this study are available from the corresponding author upon reasonable request.

## References


Angulo-Jaramillo, R., V. Bagarello, S. Di Prima, A. Gosset, M. Iovino, and L. Lassabatere. 2019. "Beerkan Estimation of Soil Transfer Parameters (BEST) Across Soils and Scales." *Journal of Hydrology* 576: 239–261. https://doi.org/10.1016/j.jhydrol.2019.06.007.

Angulo-Jaramillo, R., V. Bagarello, M. Iovino, and L. Lassabatere. 2016. *Infiltration Measurements for Soil Hydraulic Characterization*. Cham, Switzerland: Springer International Publishing.

Bagarello, V., S. Di Prima, and M. Iovino. 2014. "Comparing Alternative Algorithms to Analyze the Beerkan Infiltration Experiment." *Soil Science Society of America Journal* 78, no. 3: 724–736. https://doi.org/10.2136/sssaj2013.06.0231.

Bagarello, V., S. Di Prima, and M. Iovino. 2017. "Estimating Saturated Soil Hydraulic Conductivity by the Near Steady-State Phase of a Beerkan Infiltration Test." *Geoderma* 303: 70–77. https://doi.org/10.1016/j.geoderma.2017.04.030.

Bagarello, V., S. Di Prima, M. Iovino, and G. Provenzano. 2014. "Estimating Field-Saturated Soil Hydraulic Conductivity by a Simplified Beerkan Infiltration Experiment." *Hydrological Processes* 28, no. 3: 1095–1103. https://doi.org/10.1002/HYP.9649.

Bagarello, V., and G. Giordano. 1999. "Comparison of Procedures to Estimate Steady Flow Rate in Field Measurement of Saturated Hydraulic Conductivity by the Guelph Permeameter Method." *Journal of Agricultural Engineering Research* 74, no. 1: 63–71. https://doi.org/10.1006/jaer.1999.0437.

Bagarello, V., M. Iovino, and D. Elrick. 2004. "A Simplified Falling-Head Technique for Rapid Determination of Field-Saturated Hydraulic Conductivity." *Soil Science Society of America Journal* 68, no. 1: 66–73. https://doi.org/10.2136/sssaj2004.6600.

Bagarello, V., M. Iovino, and W. D. Reynolds. 1999. "Measuring Hydraulic Conductivity in a Cracking Clay Soil Using the Guelph Permeameter." *Transactions of the American Society of Agricultural Engineers* 42, no. 4: 957–964. https://doi.org/10.13031/2013.13276.

Braud, I., D. De Condappa, J. M. Soria, et al. 2005. "Use of Scaled Forms of the Infiltration Equation for the Estimation of Unsaturated Soil Hydraulic Properties (The Beerkan Method)." *European Journal of Soil Science* 56, no. 3: 361–374. https://doi.org/10.1111/j.1365-2389.2004.00660.x.

Carsel, R. F., and R. S. Parrish. 1988. "Developing Joint Probability Distributions of Soil Water Retention Characteristics." *Water Resources Research* 24, no. 5: 755–769. https://doi.org/10.1029/WR024i005p00755.

Di Prima, S., R. D. Stewart, M. R. Abou Najm, et al. 2021. "BEST-WR: An Adapted Algorithm for the Hydraulic Characterization of Hydrophilic and Water-Repellent Soils." *Journal of Hydrology* 603: 126936. https://doi.org/10.1016/j.jhydrol.2021.126936.

Di Prima, S., R. D. Stewart, M. Castellini, et al. 2020. "Estimating the Macroscopic Capillary Length From Beerkan Infiltration Experiments and Its Impact on Saturated Soil Hydraulic Conductivity Predictions." *Journal of Hydrology* 589: 125159. https://doi.org/10.1016/j.jhydrol.2020.125159.

Doerr, S. H., R. A. Shakesby, and L. H. Macdonald. 2009. "Soil Water Repellency: A Key Factor in Post-Fire Erosion." In *Fire Effects on Soils and Restoration Strategies, Soil Water Repellency*, edited by A. Cerdà and Peter R. Robichaud. Plymouth, England: Science Publishers.

Fuentes, C., M. Vauclin, J.-Y. Parlange, and R. Haverkamp. 1998. "Soil Water Conductivity of a Fractal Soil." In *Fractals in Soil Science*, edited by P. Baveye et al., 333–340. Boca Raton, FL: Lewis Publisher.

Haverkamp, R., F. Bouraoi, C. Zammitt, R. Angulo-Jaramillo, and J. W. Delleur. 1999. "Soil Properties and Moisture Movement in the Unsaturated Zone." In *The Handbook of Groundwater Engineering*, edited by J. W. Delleur, 5.1–5.50. Boca Raton: CRC Press.

Haverkamp, R., D. Debionne, P. Viallet, R. Angulo-Jaramillo, and D. Condapa. 2005. "Soil Properties and Moisture Movement in the Unsaturated Zone." In *The Handbook of Groundwater Engineering*, edited by J. W. Delleur, 1–59. Boca Raton: CRC Press.

Haverkamp, R., P. J. Ross, K. R. J. Smettem, and J. Y. Parlange. 1994. "Three-Dimensional Analysis of Infiltration From the Disc

Infiltrometer: 2. Physically Based Infiltration Equation." *Water Resources Research* 30, no. 11: 2931–2935. https://doi.org/10.1029/94WR01788.

Kindred, J. S., and W. D. Reynolds. 2020. "Using the Borehole Permeameter to Estimate Saturated Hydraulic Conductivity for Glacially Over-Consolidated Soils." *Hydrogeology Journal* 28, no. 5: 1909–1924. https://doi.org/10.1007/s10040-020-02149-3.

Lassabatère, L., R. Angulo-Jaramillo, J. M. Soria Ugalde, R. Cuenca, I. Braud, and R. Haverkamp. 2006. "Beerkan Estimation of Soil Transfer Parameters Through Infiltration Experiments-BEST." *Soil Science Society of America Journal* 70, no. 2: 521–532. https://doi.org/10.2136/sssaj2005.0026.

Lassabatere, L., R. Angulo-Jaramillo, J. M. Soria-Ugalde, J. Šimůnek, and R. Haverkamp. 2009. "Numerical Evaluation of a Set of Analytical Infiltration Equations." *Water Resources Research* 45, no. 12: 20. https://doi.org/10.1029/2009WR007941.

Lassabatere, L., D. Moret-Fernández, R. Angulo-Jaramillo, S. Di Prima, M. Iovino, and V. Bagarello. 2018. A new constraint on parameter beta of Haverkamp's model for 1D water infiltration. In *EGU General Assembly Conference Abstracts*4014.

Lassabatere, L., P. E. Peyneau, D. Yilmaz, et al. 2023. "Mixed Formulation for an Easy and Robust Numerical Computation of Sorptivity." *Hydrology and Earth System Sciences* 27, no. 4: 895–915. https://doi.org/10.5194/hess-27-895-2023.

Latorre, B., D. Moret-Fernández, L. Lassabatere, et al. 2018. "Influence of the β Parameter of the Haverkamp Model on the Transient Soil Water Infiltration Curve." *Journal of Hydrology* 564: 222–229. https://doi.org/10.1016/j.jhydrol.2018.07.006.

Moret-Fernández, D., and B. Latorre. 2017. "Estimate of the Soil Water Retention Curve From the Sorptivity and β Parameter Calculated From an Upward Infiltration Experiment." *Journal of Hydrology* 544: 352–362. https://doi.org/10.1016/j.jhydrol.2016.11.035.

Moret-Fernández, D., B. Latorre, M. V. López, et al. 2020. "Three- and Four-Term Approximate Expansions of the Haverkamp Formulation to Estimate Soil Hydraulic Properties From Disc Infiltrometer Measurements." *Hydrological Processes* 34, no. 26: 5543–5556. https://doi.org/10.1002/hyp.13966.

Nasta, P., L. Lassabatere, M. M. Kandelous, J. Šimůnek, and R. Angulo-Jaramillo. 2012. "Analysis of the Role of Tortuosity and Infiltration Constants in the Beerkan Method." *Soil Science Society of America Journal* 76, no. 6: 1999–2005. https://doi.org/10.2136/sssaj2012.0117n.

Nimmo, J. R., K. M. Schmidt, K. S. Perkins, and J. D. Stock. 2009. "Rapid Measurement of Field-Saturated Hydraulic Conductivity for Areal Characterization." *Vadose Zone Journal* 8, no. 1: 142–149. https://doi.org/10.2136/vzj2007.0159.

Pimentel, D. 2006. "Soil Erosion: A Food and Environmental Threat." *Environment, Development and Sustainability* 8, no. 1: 119–137. https://doi.org/10.1007/s10668-005-1262-8.

Rahmati, M., J. Vanderborght, J. Šimůnek, et al. 2020. "Soil Hydraulic Properties Estimation From One-Dimensional Infiltration Experiments Using Characteristic Time Concept." *Vadose Zone Journal* 19, no. 1: 22. https://doi.org/10.1002/vzj2.20068.

Reynolds, W. D. 2011. "Measuring Soil Hydraulic Properties Using a Cased Borehole Permeameter: Falling-Head Analysis." *Vadose Zone Journal* 10, no. 3: 999–1015. https://doi.org/10.2136/vzj2010.0145.

Reynolds, W. D. 2013. "An Assessment of Borehole Infiltration Analyses for Measuring Field-Saturated Hydraulic Conductivity in the Vadose Zone." *Engineering Geology* 159: 119–130. https://doi.org/10.1016/j.enggeo.2013.02.006.

Reynolds, W. D., and D. E. Elrick. 1990. "Ponded Infiltration From a Single Ring: I. Analysis of Steady Flow." *Soil Science Society of America Journal* 54, no. 5: 1233–1241. https://doi.org/10.2136/sssaj1990.03615995005400050006x.

Reynolds, W. D., and D. E. Elrick. 2002. "Pressure infiltrometer." In *Methods of Soil Analysis, Part 4, Physical Methods*, edited by J. H. Dane and G. C. Topp, 826–836. Madison, WI: Soil Science Society of America.

Reynolds, W. D., D. E. Elrick, and E. G. Youngs. 2002. "Single-Ring and Double- or Concentric-Ring Infiltrometers." In *Methods of Soil Analysis, Part 4, Physical Methods*, edited by J. H. Dane and G. C. Topp, 821–826. Madison, WI: Soil Science Society of America.

Stewart, R. D., and M. R. Abou Najm. 2018. "A Comprehensive Model for Single Ring Infiltration II: Estimating Field-Saturated Hydraulic Conductivity." *Soil Science Society of America Journal* 82, no. 3: 558–567. https://doi.org/10.2136/sssaj2017.09.0314.

van Genuchten, M. T. 1980. "A Closed-Form Equation for Predicting the Hydraulic Conductivity of Unsaturated Soils." *Soil Science Society of America Journal* 44, no. 5: 892–898. https://doi.org/10.2136/sssaj1980.03615995004400050002x.

Warrick, A. W. 1998. "Spatial variability." In *Enviromental Soil Physics Appendix 1D*, 665–675. California: Hillel.

White, I., and M. J. Sully. 1987. "Macroscopic and Microscopic Capillary Length and Time Scales From Field Infiltration." *Water Resources Research* 23, no. 8: 1514–1522. https://doi.org/10.1029/WR023i008p01514.

Yilmaz, D. 2021. "Alternative α* Parameter Estimation for Simplified Beerkan Infiltration Method to Assess Soil Saturated Hydraulic Conductivity." *Eurasian Soil Science* 54, no. 7: 1049–1058. https://doi.org/10.1134/S1064229321070140.

Yilmaz, D., S. Bouarafa, P. E. Peyneau, R. Angulo-Jaramillo, and L. Lassabatere. 2019. "Assessment of Hydraulic Properties of Technosols Using Beerkan and Multiple Tension Disc Infiltration Methods." *European Journal of Soil Science* 70, no. 5: 1049–1062. https://doi.org/10.1111/ejss.12791.

Yilmaz, D., L. Lassabatere, R. Angulo-Jaramillo, D. Deneele, and M. Legret. 2010. "Hydrodynamic Characterization of Basic Oxygen Furnace Slag Through an Adapted BEST Method." *Vadose Zone Journal* 9, no. 1: 10. https://doi.org/10.2136/vzj2009.0039.

Yilmaz, D., L. Lassabatere, D. Moret-Fernandez, M. Rahmati, R. Angulo-Jaramillo, and B. Latorre. 2023. "Soil-Dependent β and γ Shape Parameters of the Haverkamp Infiltration Model for 3D Infiltration Flow." *Hydrological Processes* 37, no. 6: 10. https://doi.org/10.1002/hyp.14928.

Youngs, E. G., P. B. Leeds-Harrison, and D. E. Elrick. 1995. "The Hydraulic Conductivity of Low Permeability Wet Soils Used as Landfill Lining and Capping Material: Analysis of Pressure Infiltrometer Measurements." *Soil Technology* 8, no. 2: 153–160. https://doi.org/10.1016/0933-3630(95)00016-X.

Zhang, J., T. Lei, Z. Yin, Y. Hu, and X. Yang. 2017. "Effects of Time Step Length and Positioning Location on Ring-Measured Infiltration Rate." *Catena* 157: 344–356. https://doi.org/10.1016/j.catena.2017.05.013.